Influence of low-frequency quasar 3C 273 radio spectrum on X-ray emission of its kiloparsec jet

M. S. Mykhailova[1], *V. M. Kontorovich*[1,2]

[1]Institute of Radio Astronomy of NAS of Ukraine, Chervonopraporna st., 4, 61002, Kharkiv, Ukraine
[2]V. N. Karazin Kharkiv National University, Svoboda sq., 4, 61077, Kharkiv, Ukraine
aniramtiger@gmail.com

In this paper the X-ray emission spectrum from the nearest to the quasar 3C 273 inner jet knot A was investigated by the kinetic equation method. It is shown that the inverse Compton scattering of the quasar radio emission is responsible for the X-ray emission of the knot. Under certain conditions it is possible to determine the position of the low-frequency break in the spectrum of the quasar using the X-ray radiation of its jet.

Introduction

The kiloparsec scale jet [5] of the nearest quasar 3C 273 [3] is observed with the high angular resolution ($\sim 0.1''$) within a wide range of frequencies [6, 11, 4, 10, 14]. The jet has regions of high radiation intensity – knots, which correspond to the regions of relativistic electron acceleration [3]. The knot structure of the jet has a characteristic feature: the intensity of the knots in the radio range increases with the distance from the quasar and reaches a maximum in the last knot corresponding to the bow shock wave [10]. In the optical band the knots have almost equal brightnesses. In the X-rays range, conversely, the intensity of the three nearest to the quasar knots decreases with the distance from the core and remains constant for the long-distance knots[1] [6, 11]. Such intensity distribution lead us to the idea that the X-rays of the distant jet knots have been formed by the inverse Compton scattering (ICS) on relict (background) radiation [1], while the X-ray emission of inner knots is produced by ICS on the radiation of the quasar[2]. From a simple estimation it is clear that the energy density of emission of the central source with luminosity $L \sim 10^{47}$ erg/s becomes comparable with the energy density of the cosmic microwave background at the distance of a few tens kpc, that takes place for the jet of the quasar 3C 273. Competition of the scattering mechanisms allowed to determine the angle between the jet and the image plane [7]. Radio and optical knot emission was associated with the synchrotron mechanism [3]. Due to the scale set by the relict radiation it became possible to determine the values of the magnetic field and concentration of relativistic electrons in the distant knots [7] without any additional assumptions comparing the synchrotron radiation with ICS.

In this paper we present the detailed analysis of ICS in the nearest to the quasar knot A, based on the first principles and using the kinetic equation method. It is shown that ICS of the quasar radiation is responsible for the X-ray emission of the knot. We have assumed the power-law electron energy distribution with spectral index $\gamma \approx 2.2$ based on the radio and optical observational data. Correspondingly, the scattering on the most high-energy electrons (with Lorentz-factor $\Gamma \sim 10^6 - 10^7$) gives the main contribution to X-ray radiation of the *Chandra* range. Hence, the low radio frequency quasar photons with frequencies $\omega \sim 10^8$ s^{-1} (and lower) have been scattering in this process. It is shown that the X-ray spectral index coincides with the spectral index of the scattered low-frequency radiation. Thus, one can get an information about low-frequency quasar spectrum by analyzing the X-ray data. Under certain conditions it is possible to determine the position of the low-frequency break in the spectrum of the quasar using the X-ray radiation of its jet.

[1]With the exception of the last knot, where X-ray emission is below of the threshold of observation.
[2]It is considered as radiation of the quasar and its parsec scale jets together with their environment.

The flux density for ICS on the electrons with power-law spectra

The kinetic equation for ICS is

$$\frac{d}{dz}N\left(\mathbf{k}'\right)=\iint\left(1-\beta\,\cos\psi\right)\sigma\left(\mathbf{p},\mathbf{p}',\mathbf{k},\mathbf{k}'\right)f\left(\mathbf{p}\right)N\left(\mathbf{k}\right)\,d^3p'\,d^3p\,d^3k, \tag{1}$$

where parameters after scattering are marked with the strokes, $N\left(\mathbf{k}\right)$ is the photon distribution function (DF), $f\left(\mathbf{p}\right)$ is the electron energy DF, z is the axis along line of sight. The equation was obtained from relativistic invariant kinetic equation [9]. Induced scattering processes are neglected. The differential cross-section is

$$\sigma\left(\mathbf{p},\mathbf{p}',\mathbf{k},\mathbf{k}'\right)=\frac{r_e^2}{2}\frac{m^2c^4}{E\,E'}\frac{\hbar c^2}{\omega\,\omega'\left(1-\beta\,\cos\psi\right)}G\left(\xi,\xi'\right)\delta\left(\mathbf{p}+\hbar\mathbf{k}-\mathbf{p}'-\hbar\mathbf{k}'\right)\delta\left(E+\hbar\omega-E'-\hbar\omega'\right), \tag{2}$$

where r_e, m, E and $\beta\,c$ are the classical radius, the mass, the energy and the velocity of the electron, correspondingly,

$$G\left(\xi,\xi'\right)=\left(1/\xi-1/\xi'\right)^2+2\left(1/\xi-1/\xi'\right)+\xi/\xi'+\xi'/\xi, \tag{3}$$

$$\xi=E\hbar\omega\left(1-\beta\cos\psi\right)/\left(m^2c^4\right),\qquad \xi'=E\hbar\omega\left(1-\beta\cos\varphi\right)/\left(m^2c^4\right),$$

ψ, φ, θ are the angles between momenta of interacting particles (Fig. 1). The angle between jet and line of sight is $\theta\approx 30^\circ$ [7]. The delta-functions reflect the energy and momentum conservation laws during the scattering. Both the electron energy DF

$$f\left(E\right)=\mathcal{K}\,E^{-\gamma},\quad E_{\min}<E<E_{\max} \tag{4}$$

and DF of initial radiation obtained from quasar observation data have been approximated by power-law

$$N\left(\omega\right)\equiv\frac{4\pi\omega^2}{c^3}N\left(\mathbf{k}\right)=\frac{QD^2}{c\hbar R^2}\,\omega^{-(\alpha+1)}\,, \tag{5}$$

where $\mathcal{K}$ and Q are the normalization constants, D is the distance to 3C 273, R is the distance from the quasar to knot A, γ is the spectral index of electron DF in the knot A, α is the spectral index of quasar photons.

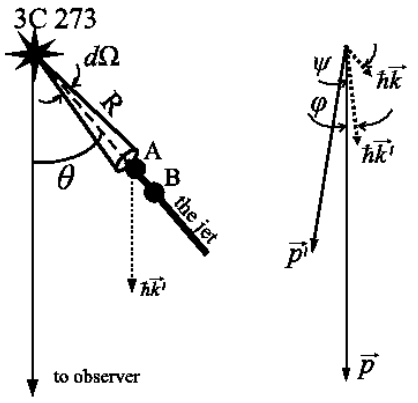

Figure 1: Scheme of ICS in the jet knot A. $\vec{p}$, $\vec{p}\,'$, $\hbar\vec{k}$, $\hbar\vec{k}\,'$ are the electron and photon momenta before and after scattering correspondingly.

Taking into account the substitutions (2)-(5) into expression (1) the integration over the dp' is performed using δ-function. From the kinetic equation one can find:

$$N\left(\mathbf{k}'\right)=\int\!\!\int\frac{r_e^2 l_z}{(4\pi)^2}\frac{c^2QD^2}{2\hbar R^2}\frac{\mathcal{K}\,m^2c^4G\left(\xi,\xi'\right)\delta\left(\omega-\omega'\frac{1-\beta\,\cos\varphi}{1-\beta\,\cos\psi}\right)}{\left(1-\beta\,\cos\psi\right)}\,\omega^{-\alpha-2}\omega'^{-1}E^{-\gamma-2}d\Omega_p\,dE\,d\Omega\,d\omega, \tag{6}$$

where l_z is the knot size along the line of sight, Ω and Ω_p are the solid angles of initial photons and electrons correspondingly. Flux density of the scattered radiation after integration over $d\omega$ with δ-function and over $d\Omega_p$ is:

$$F\left(\omega'\right) = \frac{r_e^2 l_z}{2\left(\alpha+1\right)} \frac{QD^2}{R^2} \left(mc^2\right)^{1-\gamma} \mathcal{K}\, \Delta\Omega\, \Delta\Omega_{k'} \left[2\left(1-cos\theta\right)\right]^{\alpha+1} \omega'^{\,-\alpha} \int^{\Gamma_{\max}} \Gamma^{2\alpha-\gamma} d\Gamma, \tag{7}$$

where $\Delta\Omega_{k'}$ is the solid angle of knot A. For integration over $d\Omega_p$ we used $\cos\psi \approx \cos\theta$. The spectral indexes are known from observations and have values $\alpha \approx 0.7$, $Q \approx 1 \cdot 10^{-11}$ [13] and $\gamma \approx 2.2$ [2]. The normalization constant $\mathcal{K}$ can be expressed in terms of electron concentration n_e in the knot $\mathcal{K}\left(mc^2\right)^{\gamma-1} = n_e\left(\gamma-1\right)\Gamma_{min}^{\gamma-1}$ which is known [7]. Hence, for the flux density we have

$$F\left(\omega'\right) = \frac{r_e^2 l_z\; n_e\left(\gamma-1\right)\; QD^2}{2\left(\alpha+1\right)\left(2\alpha+1-\gamma\right)R^2} \Delta\Omega\, \Delta\Omega_{k'} \left[2\left(1-cos\theta\right)\right]^{\alpha+1} \Gamma_{\max}^{2\alpha+1-\gamma} \cdot \left(\omega'\right)^{\,-\alpha}. \tag{8}$$

We see that the electrons having the largest Lorentz-factor scatter the photons most efficiently (Fig. 2, 3). This result confirms our assumption that X-rays from the knot A are produced by ICS on the central source radiation.

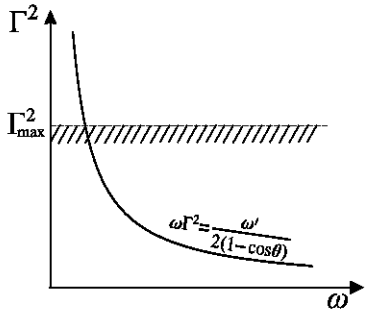

Figure 2: The integration region for case of both power-law photon and electron spectra.

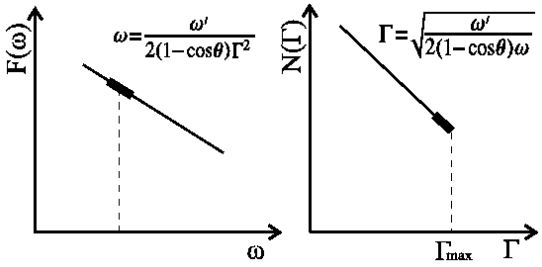

Figure 3: Scheme of photon and electron energy distribution (logarithmic scale). The bold lines mark the parts of DFs, which are the most efficient in scattering.

The maximum Lorentz-factor of electrons $\Gamma_{\max} \approx 10^6$ can be obtained from the flux densities data [14] at corresponding frequencies. On the other hand, the observed optical emission, that has the synchrotron nature [10], gives for the electron Lorentz-factor $\sim 10^7$ for the magnetic field $H \approx 10^{-6}$ Gs [7]. This contradiction may be resolved by integrating not to the maximum electron energy but to the low frequency spectrum of the quasar (see Fig. 4, 5).

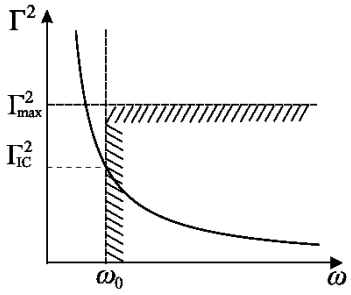

Figure 4: The integration region for case of low-frequency break.

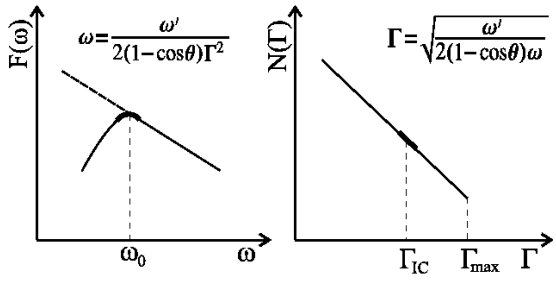

Figure 5: Scheme of fall-off photon and electron energy spectra.

Hence, the fall-off [12] in the spectrum of the central source may play the primary role. This fall-off (or break) can be produced, for example, by synchrotron self-absorption or thermal plasma absorption. In this

case the photons having the fall-off frequency are scattered into *Chandra* range on the electrons that have Lorentz-factor smaller then the maximum one (Fig. 5). Therefore we have the integral limit from the photon spectrum. Using in (1) δ-function which reflects the energy conservation law and the mentioned substitutions we have for DF of the scattered photons

$$N\left(\mathbf{k}'\right) = \frac{r_e^2 l_z}{8\pi\left(\gamma+1\right)} \frac{c^2 Q D^2}{\hbar R^2} \left[2\left(1-\cos\theta\right)\right]^{\frac{\gamma+1}{2}} \Delta\Omega\, \mathcal{K}\, \left(mc^2\right)^{1-\gamma}\, \omega'^{-\frac{\gamma+5}{2}} \int\limits_{\omega_0} \omega^{-\frac{2\alpha+3-\gamma}{2}}\, d\omega, \tag{9}$$

where ω_0 is the frequency of fall-off. As $2\alpha+1-\gamma>0$, then the flux density becomes

$$F\left(\omega'\right) = \frac{r_e^2 l_z\, n_e\left(\gamma-1\right)\, Q D^2}{\left(\gamma+1\right)\left(2\alpha+1-\gamma\right) R^2} \left[2\left(1-cos\theta\right)\right]^{\frac{\gamma+1}{2}} \Delta\Omega\, \Delta\Omega_{k'}\, \omega_0^{-\frac{2a+1-\gamma}{2}}\, \omega'^{-\frac{\gamma-1}{2}} \tag{10}$$

Thus, we have found that the low frequency fall-off of quasar radiation occurs at the frequency $\omega_0 \approx 10^8$ Hz. Note, the results of this consideration are sensitive to the angular dependence of the cross-section (see discussion for two different assumptions in [8]).

Another explanation may be based on the assumption that the optical emission of the knot A is produced by ICS of the central source radiation. In this case the flux density of the optical emission from the knot A may be obtained using (8) and data from [14]. The observed and calculated flux densities are in a good agreement.

Conclusions

We considered ICS of power-law quasar radiation on the power-law relativistic electrons in the nearest to the quasar 3C 273 jet knot A. The main contribution to X-ray radiation under some conditions is given by the high-energy electron scattering, which confirms the assumption about ICS. The maximum Lorentz-factor of the electrons was estimated. It turns out, that in some cases it is not sufficient to produce the optical synchrotron emission observed in the jet knot A. One of the alternative explanations deals with restriction in the spectrum of the central source from the low frequency break. In this case ICS is produced by the electrons with Lorentz factor smaller than the maximum.

Hence, we found the remarkable possibility to make some conclusions about low frequency spectrum of sources similar to 3C 273 under certain conditions and estimate the position of low frequency break using the X-ray observational data.

References

[1] Bannikova E. Yu., Kontorovich V. M. Space Science and Technology, V. 5/6, pp. 153-157 (2003)

[2] Conway R. G., Garrington S. T., Perley R. A., Biretta J. A. Astron. & Astrophys., V. 267, pp. 347-362 (1993)

[3] Courvoisier T. J.-L. Astron. & Astrophys. Rev., V. 9, pp. 1-32 (1998)

[4] Jester S., Röser H.-J., Meisenheimer K. et al. Astron. & Astrophys., V. 431, pp. 477-502 (2005)

[5] Harris D. E. et al. `http://hea-www.harvard.edu/XJET/`

[6] Marshall H. L., Harris D. E., Grimes J. P. et al. Astrophys. J., V. 549, pp. 167-171 (2001)

[7] Mikhailova M. S., Bannikova E. Yu, Kontorovich V. M. Astron. Rep., V. 54, pp. 481-488 (2010)

[8] Mykhailova M. S., Kontorovich V. M. Problems of Atomic Science and Technology, V. 4, pp. 149-154 (2010)

[9] Nagirner D. I. Radiation processes in astrophysics, SPb University Press, Saint-Petersburg (2007)

[10] Röser H.-J., Meisenheimer K. Astron. & Astrophys., V. 252, pp. 458-474 (1991)

[11] Sambruna R. M., Urry C. M., Tavecchio F. et al. Astrophys. J., V. 549, pp. 161-165 (2001)

[12] Slish V. I. Nature, V. 199, p. 682 (1963)

[13] Soldi S., Türler M., Paltani S. et al. Astron. & Astrophys., V.486, pp. 411-425 (2008)

[14] Uchiyama Ya., Urry C., Cheung C. et al. Astrophys. J, V. 648, pp. 910-921 (2006)